

DISTRIBUTION OF GENERATED FRICTION HEAT AT WHEEL-RAIL CONTACT DURING WHEEL SLIPPING ACCELERATION

by

Miloš S. MILOŠEVIĆ*, **Milan S. BANIĆ**, **Dušan S. STAMENKOVIĆ**,
Vukašin D. PAVLOVIĆ, **Miša M. TOMIĆ**, and **Aleksandar V. MILTENOVIĆ**

Faculty of Mechanical Engineering, University of Nis, Nis, Serbia

Original scientific paper
DOI: 10.2298/TSCI16S5561M

This paper presents an innovative method for determining the distribution of the friction generated heat from the contact of a locomotive wheel and rail, as well as the heat partition factor, during wheel slipping of an accelerating locomotive. The new method combines the finite element analysis simulation and experimental determination of the temperature distribution in a downsized model of a wheel and rail. As a result of a virtual experiment by the finite element analysis, an empirical dependence between the temperature distribution and the heat partition factor was established. The determination of the dependence enabled finding of the exact value of the heat partition factor by the optimization procedure based on matching temperatures obtained by the virtual and real experiment.

Key words: *friction heat generation, heat partition factors, wheel-rail contact, slipping acceleration, sliding*

Introduction

Problems relating to the determination of the friction generated heat, temperature distribution and heat partition factor in the wheel-rail contact are well known in scientific circles, and a great number in studies of the fields of railway and tribology deal with them. Those problems are related to rolling contact fatigue (RCF) and wear of the wheel-rail system. Relative slip at the wheel-rail interface leads to an increase in temperature causing thermal softening of the steel that can even lead to its metallurgical transformation. Furthermore, thermal stresses cause occurrence of residual stresses which contribute to the propagation of cracks in materials [1].

Knothe and Liebelt [2] presented an approach that used a combination of Green's functions and the Laplace transform method to obtain solutions for surface temperatures, maximum contact temperatures and temperature fields for sliding systems. An appropriate procedure was provided for the wheel-rail system in this study. Furthermore, Ertz and Knothe [3] showed that the heat flow in a wheel-rail contact with smooth surfaces was 1-D. The authors presented some methods for the calculation of contact temperatures, and concluded that the maximum surface temperature could be estimated with the flash temperature formula of Blok, while the case of Hertzian contact could be investigated with the polynomial approximation. Gallardo-Hernandez *et al.* [4] measured temperatures in a twin-disc simulation of wheel-rail contact. For that purpose, a thermal camera was used. Obtained temperatures were

* Corresponding author; e-mail: mmilos@masfak.ni.ac.rs

compared with temperatures derived using analytical models, which equated the frictional heat generated in the contact, and good correlation was found between them. Thermal stresses for frictional contact at wheel-rail systems were investigated by Fischer *et al.* [5]. Using the Laplace transform technique, an analytical solution for the temperature field produced by sliding contact on the surface of a half plane, was presented.

Many authors used numerical simulations to research the heat generation during friction between two bodies, especially in the case of wheel-rail contact. Sinha *et al.* [6] considered the transient case of a block sliding across two fixed walls. Belhocine *et al.* [7-9] investigated structural and contact behaviors of full and ventilated brake disc and pads during the braking phase with and without thermal effects. Milošević *et al.* [10] performed analytical and numerical modeling of thermal effects during long-term braking of locomotive for maintaining a constant speed on a down-grade railroad. Stefanacu *et al.* [11] analyzed the frictional heating phenomenon using the finite element method for frictional dampers used as earthquake protective systems. Masoudi *et al.* [1, 12] and Salehi *et al.* [13] used 3-D finite element analyses for simulation of in railway wheels, as well as the effect of residual stresses on cracks growth and wheel life.

For the wheel-rail contact, Miltenović *et al.* [14] used the ANSYS software to obtain the wheel-rail temperature distribution in different sliding scenarios. During the analysis, the authors assumed that the equal amounts of the generated heat flew to both bodies in the contact, *i. e.* the heat partition factor value was assumed to be 0.5. Fischer *et al.* [15] investigated the flash temperature in an asperity of the rail due to the wheel-rail rolling contact. They derived a new heat partition factor in cases of frictional heating and heating due to plastic deformations. Spiriyagin *et al.* [16] proposed minimizing the wear between the wheel flange and the rail gauge by the lubricant implementation. Modeling the temperature process in the contact and using some experimental data as an input for the computation, the obtained results of the numerical calculation of temperature were used for making the correct choice of the lubricant type. Vakkalagadda *et al.* [17] proposed a three step hybrid approach for determination of wheel running temperatures, which included a model of a running train for estimation of heat generation rates, a 2-D boundary element method for estimation of heat partition and a finite element method for estimation of wheel temperatures taking inputs from the train running model and the boundary element method.

The analysis of the considered literature sources leads to the observation that the majority of authors during their researches were made the following two assumptions: first that the overall energy generated by friction is transformed into heat, and second that the equal amounts of the generated heat are transferred to the both bodies in the contact. Although there may be disagreements about the exact mechanism of the energy transformation, most tribologists agree that nearly all of the energy dissipated in frictional contacts is transformed into heat [18]. Due to a number of factors which influence the frictional heat generation as well as different geometry and thermal properties of bodies in contact, it is not justified to assume that both bodies receive the equal heat flow. To determine the heat partitioning, it is necessary to establish a model of contact and to solve governing partial differential equations along with the interface and boundary conditions. Due to the complexity of the contact model, it is usually reduced to 1-D or 2-D representation in order to achieve the solution of the heat partitioning problem.

This paper presents an innovative approach to the determination of the parameter for partitioning of the friction generated heat by combining a real experiment on a downsized model with numerical virtual experiment results. The simple experiment provides the deter-

mination of temperature distribution for tribological conditions of the wheel-rail contact. With the 3-D direct coupled structural-thermal numerical simulation, which resembles the performed experimental set-up, the heat partition factor is varied in order to match temperature distribution obtained numerically with temperature distribution obtained by performing experiment on the downsized model. The matching of noted temperature distributions gives an exact value of the heat partitioning factor for different tribological conditions, thus enabling more accurate simulations of the wheel-rail contact.

Friction and frictional heating

Friction occurs whenever two solid bodies slide against each other. During this process, mechanical energy transforms into internal energy or heat, which causes increasing of the temperature of the sliding bodies. Depending on the sliding conditions mechanism by which this energy transformation occurs may vary. Also, the exact location of that transformation usually is not known for certain. It is known that solid friction and related frictional processes, including frictional heating, are concentrated within the real area of contact between two bodies in relative motion. Most of the authors already agree that nearly all of the energy dissipated in frictional contacts is transformed into heat. Increases in temperatures of the sliding bodies occur due to the energy dissipation, also called frictional heating.

In the case where two bodies slide against each other, where the body 1 is moving with velocity v_1 relative to the contact area and the body 2 is moving with velocity v_2 relative to the same contact area, the rate of total energy dissipated in the sliding contact is determined by the friction force, and the relative sliding velocity. If it is assumed that all of this energy is dissipated as heat on the sliding surfaces within the real area of contact, then the rate of heat generated per unit area of contact, q_t , is given by:

$$q_t = \mu p \Delta v \quad (1)$$

where μ is the coefficient of friction, p – the contact pressure, and $\Delta v = v_2 - v_1$ – the relative sliding velocity. This heat generated by friction is distributed through both bodies in contact and distribution can be calculated by Fourier's law.

Fourier's law for heat conduction in an isotropic solid which is moving with the velocity v may be written as is shown:

$$\nabla k \nabla T + \dot{Q} = \rho C \frac{dT}{dt} = \rho C \left(\frac{\partial T}{\partial t} + v \nabla T \right) \quad (2)$$

where \dot{Q} is the internal heat generation rate per unit volume, k – the thermal conductivity, ρ – the density, and C – the specific heat.

Since there is no internal heat generation in the case relating to this paper, and when k is uniform and constant, eq. (2) can be written:

$$k \nabla^2 T = \rho C \left(\frac{\partial T}{\partial t} + v \nabla T \right) \quad (3)$$

or shorter:

$$\nabla^2 T = \frac{1}{\kappa} \frac{dT}{dt} \quad (4)$$

where $\kappa = k/\rho C$ is the thermal diffusivity.

Frictional heating and the resulting contact temperatures can have an important influence on the tribological behavior and failure of sliding components. Surface and near-surface temperatures can become high enough to cause changes in the structure and properties of the sliding materials, oxidation of the surface and possibly even melting of the contacting solids. These temperature increases can often be responsible for changes in the friction and wear behavior of the material [18]. This is very important in railway because of the fact that sliding of the wheel relative to the rail occurs frequently in cases when a locomotive starts its motion or accelerates from one velocity to another [19]. The motion of a railway vehicle wheel on the rail is usually considered as a purely rolling, but in practice often rolling and sliding occur simultaneously. Hence, sliding of the wheel on the rail mainly performs in cases of vehicle accelerating or braking.

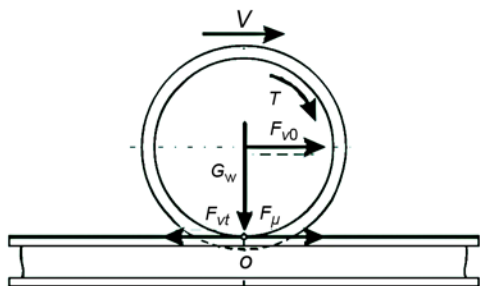


Figure 1. Torque and friction force in wheel-rail contact

Figure 1 shows the realization of the traction force F_{v0} according the slip resistance force *i. e.* the friction force F_{μ} . The drive torque T represents the moment of the forces $F_{v0} - F_{vt}$. The horizontal rail reaction force F_{μ} (the friction force) is generated under the influence of the vertical wheel load G_w , and it opposes to the force of the traction torque F_{vt} balancing it. So, the rotation around the point O is performed under the force F_{v0} , and the vehicle is moving.

Hence, the movement of the wheel is performed by means of friction. Because of the friction of the wheel-rail contact the heat

is generated. It is important to know the process of the heat distribution in the contact area in order to achieve energy efficiency and safety of railway transport.

Innovative method for determination of heat partition factor

As already noted, the analytical or numerical determination of the heat partition factor is very hard as it requires the definition of the contact model for a specific tribological case, as well as solving a complex system of governing partial differential equations. Therefore, in this paper, an innovative method was proposed to determine the heat partition factor of the contact of a locomotive wheel and rail.

The heat partition factor can be determined by a combination of a virtual experiment based on a finite element simulation and a real experiment on a downsized model of the wheel-rail contact. The wheel-rail contact could be downsized to a smaller model with the same tribological properties in order to enable the execution of a simple experiment in laboratory conditions. The goal of the experiment is to capture the temperature distribution of the downsized model for identical tribological conditions. It is then possible to set up a numerical simulation, which resembles the performed experimental set-up, in order to perform virtual experiments for different values of the heat partition factor for determination of the temperature distribution of the wheel and the rail. It is then possible to define an empirical mathematical relation between the heat partition factor and temperature distribution results. Inserting experimental temperature results of the downsized wheel-rail model in the empirical mathematical relation, obtained via the virtual experiment by finite element method, it is possible to

calculate the exact value of the heat partition factor. The calculation can be made with an optimization procedure aimed to match temperature data from the real experiment and temperature data calculated by the empirical mathematical model. The algorithm of the procedure is shown in fig. 2.

Experiment on downsized wheel-rail model

Figure 3 shows a schematic representation of the experimental set-up of a downsized wheel-rail model while the experimental set-up is shown in fig. 4. The rail and wheel of a locomotive were downsized in dimensions ten times for the wheel-rail model and the wheel and rail were made from the same materials and with the same hardness and roughness as in reality (the material of the rail was steel 42CrMo4 and of the wheel was steel R260Mn, the hardness of the rail was 28HRC and of the wheel was 20HRC, the roughness of the rail was N6 and of the wheel was N7). The goal of such approach was to obtain the similar tribological conditions as in actual contact of the lo-

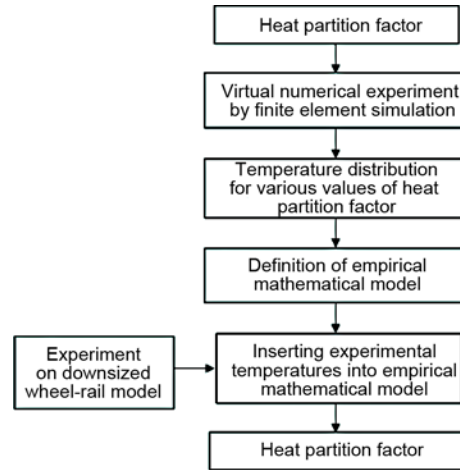


Figure 2. Procedure algorithm

Figure 3. Schematic representation of measuring set-up

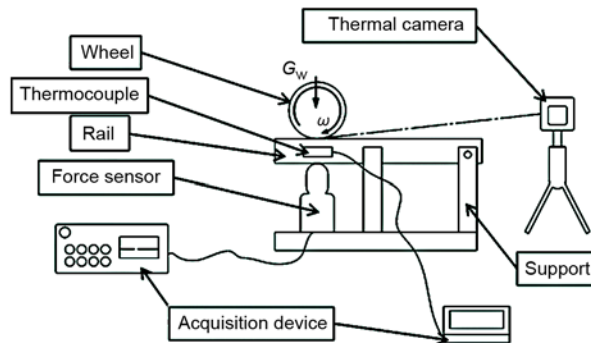


Figure 4. Experimental measuring set-up

comotive wheel and rail. For the experimental purpose, the downsized wheel was attached to the shaft of a milling cutter, while the downsized rail was put on a support. One end of the rail was joined by a rotational joint to the support while the opposite one was free to move vertically. Below the free end of the rail the force sensor HBM U9C 5kN was installed and connected to HBM Quantum X measurement data acquisition system. This combination of the rotational joint and the free end of the rail enabled the measurement of the force with which the wheel loaded the rail. The value of the loading force was calculated in such a way that the contact pressure should be the same as in the case of the actual locomotive wheel and rail contact. To achieve the contact pressure of $p \approx 600$ MPa the loading force was calculated to the value of $G_w = 1000$ N. The calculated loading force was exerted on the shaft by lifting the work desk of the milling cutter. As the slip ratio is about 10% during wheel sleeping acceleration [13] the shaft speed was adjusted to $\omega = 22$ rpm, which corresponded to the tangential velocity of about $v = 540$ m/s.

The wheel and rail were painted in a matte black paint in order to simulate a black body with the emissivity value of $\varepsilon = 1$. Thermal imaging was used to obtain the temperature distribution of the downsized wheel-rail model, while thermocouple SA1XL (surface mounted – type K) was attached to the rail to control

Table 1. Thermal camera parameters used during thermal imaging

Thermal imaging parameter	Value
Emissivity	1
Ambient temperature	20 °C
Apparent reflected temperature	20 °C
Humidity	76%
Distance	1 m



Figure 5. Temperature distribution of downsized model of wheel-rail contact
(for color image see journal web-site)

the results obtained via thermal imaging. The thermocouple was connected to the NI 9211 acquisition module. For thermal imaging, the FLIR E50 infrared camera with the resolution of 320×240 was used. In order to have absolute accuracy of thermal imaging, the values of the ambient temperature and local humidity were measured as well as the distance of the wheel-rail model to the camera. The experiment was performed during the night in complete darkness in order to avoid reflections. The set-up thermal camera parameters for the experiment are shown in tab. 1.

Figure 5 shows the results of thermal imaging. From the image and dimensions of the wheel-rail model, it is calculated that the distance between two pixels in horizontal, z-direction, is 0.9 mm and that distance from two pixels in vertical, y-direction, is 1.0715 mm. The center of the local coordinate system was established in the middle of the imagined contact line between the rail and the wheel. The orientation of the principal axis is shown in fig. 6. In FLIR Tools software, eight measuring points on the rail were defined and temperature readings were obtained for noted points. The distance between the points and their position

on the rail is obtained by counting the pixels on the image. Temperature readings were obtained 1.5 seconds from the start of the experiment. The experiment was performed five times and temperature readings were averaged in measuring points. Table 2 shows the obtained av-

eraged temperature readings and the positions of measuring points in relation to the local coordinate system.

Numerical simulation

The numerical analysis was performed in ANSYS Workbench software as the direct coupled transient structural-thermal analysis. The set-up of the analysis reflects the experimental set-up as described in the previous section. The model load and boundary conditions were defined by using of three joints in order to account for wheel rotation, apply the wheel pressure onto rail, and to fix the rail to the ground. Heat transfer with surroundings was defined as convection from all surfaces with the heat transfer coefficient of $10 \text{ W/m}^2\text{K}$. It was necessary to define convection via the named selection and command interface as ANSYS Workbench currently does not have the graphical user interface for the direct structural-thermal coupling.

The material properties used for the analysis are given in tab. 3. These values were considered constant during the analysis as the simulation time was short (1.5 seconds, the same as in the experiment) and expected temperatures were below $50 \text{ }^\circ\text{C}$.

In order to perform the coupling of the thermal and structural field higher order, SOLID226 [20] was used for meshing of the model. To increase the accuracy of finite element computations, the contact of the wheel and rail was meshed with a higher density mesh as shown in fig. 6. The model consists of 118711 nodes which form 24788 finite elements.

The contact between the wheel and rail was defined as a frictional contact, with the friction coefficient value of $\mu = 0.35$ [14] which corresponds to friction during wheel slipping acceleration of a locomotive. The contact was modeled via ANSYS CONTA174 and TARGE170 elements [20] that correspond to the wheel as a contact surface and the rail as a target surface. The contact was treated as a symmetric pair and during simulation the augmented Lagrange formulation was adopted. The contact stiffness was updated for each solution iteration automatically.

A mesh size sensitivity test was performed to obtain confidence in accuracy of finite element simulations. It was assumed that the simulation results are insensitive to mesh size if the difference in equivalent stress and total deformation in two adjunct meshes is below 5%.

Table 2. Temperature results in defined points on the rail

1 \equiv SV1	$x = 2, y = -1.0715, z = 0$	47.3
2 \equiv SV2	$x = 2, y = -2.143, z = 0$	41
3 \equiv SV3	$x = 2, y = -3.2145, z = 0$	37.4
4 \equiv SV4	$x = 2, y = -4.286, z = 0$	34.9
5 \equiv SH1	$x = 2, y = -1.0715, z = -0.9$	44.7
6 \equiv SH2	$x = 2, y = -1.0715, z = -1.8$	43.3
7 \equiv SH3	$x = 2, y = -1.0715, z = 0.9$	43.2
8 \equiv SH4	$x = 2, y = -1.0715, z = 1.8$	41

Table 3. Parameters used for heat transfer simulation

Parameter	Value
Stefan-Boltzmann constant [$\text{Wm}^{-2}\text{K}^{-4}$]	$5.67 \cdot 10^{-8}$
Steel specific heat capacity [$\text{Jkg}^{-1}\text{K}^{-1}$]	434
Steel conductivity coefficient [$\text{Wm}^{-1}\text{K}^{-1}$]	60.5
Convective heat transfer coefficient from steel to air [$\text{Wm}^{-2}\text{K}^{-1}$]	10

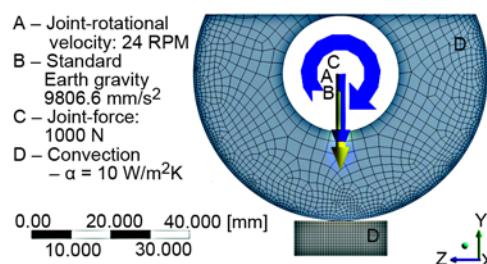


Figure 6. Numerical analysis set-up

Maximum mesh skewness of the model was 0.7 which proved mesh quality and thus provided confidence in simulation results. The analysis was performed with a fixed time step of 0.01 seconds. It was determined that the selected time step was sufficient to obtain insensitivity of results from the size of the time step.

The governing equations were solved with the sparse equation solver and full Newton method for treating the non-linear contact equations. The solver was instructed to use large deformations theory during the solution as it was assumed that non-linear solution was more accurate. As the solution was already non-linear due to the non-linear frictional contact there was computational performance penalty.

Furthermore, solver was instructed to calculate the frictional generated heat during solution by issuing of command in the contact set-up. The rate of frictional dissipation in contact elements in ANSYS is evaluated using the frictional heating factor and is given by equation (5) [20]:

$$q = FHTG \tau v \quad (5)$$

where q is the total heat generated, $FHTG$ – the fraction of the frictional dissipated energy converted into the heat, τ – the frictional stress, and v – the sliding rate. During the analysis, the frictional dissipated energy fraction is defaulted to 1, *i. e.* it is assumed that all the energy generated in frictional interaction is transferred into thermal energy. The heat generated on the two surfaces involved in the friction interaction is divided up by the following equations [20]:

$$q_w = FWGT q \quad (6)$$

$$q_r = (1 - FWGT) q \quad (7)$$

where q_w and q_r represent the heat dissipated to the wheel side and the heat dissipated to the rail side, respectively, and $FWGT$ is the heat partition factor.

Based on the previously described finite element model, a virtual experiment was defined by using of ANSYS design of experiments module as a central composite design. In total, five virtual experiments were defined with different values of $FWGT$ *i. e.* the heat partition factor. The temperature data was monitored in eight points on the rail with the same coordinates as the points defined in the experiment shown in Chapter *Experiment on downsized wheel-rail model*, tab. 2. By solving the noted virtual experiments, a set of numerical results of temperature data for monitored points was obtained as shown in tab. 4.

Table 4. Virtual experiment set-up and results

	Point N°							
	1 ≡ SV1	2 ≡ SV2	3 ≡ SV3	4 ≡ SV4	5 ≡ SH1	6 ≡ SH2	7 ≡ SH3	8 ≡ SH4
<i>FWGT</i> value	Temperature [°C]							
0.1	47.886	39.547	34.61	31.316	43.709	37.784	43.555	37.769
0.3	44.341	37.105	32.862	30.023	40.735	35.608	40.567	35.565
0.5	40.765	34.672	31.113	28.731	37.7	33.411	37.611	33.393
0.7	37.179	32.247	29.362	27.438	34.656	31.209	34.638	31.221
0.9	33.572	29.81	27.612	26.146	31.637	29.021	31.628	29.022

The response surface which defined the dependence of temperature data on the rail from the heat partition factor was determined by Kriging or Wiener-Kolmogorov prediction which gave an optimal interpolation based on regression against observed z values of surrounding data points, weighted according to spatial covariance values [21]. The noted prediction gave almost a perfect fit between the predicted values of temperature in points as the coefficient of the determination value was $R^2 = 1$ and the root mean square error was below 10^{-11} . The comparison of predicted values in monitoring points with temperature data in the same points obtained by virtual experiment is shown in fig. 7. The points designations in figure correspond to point designations in tabs. 2 and 4.

From fig. 8, it is clear that there is a linear dependence between the value of the heat partition factor and the value of temperature in the monitoring points. As there are eight different linear dependences for eight monitoring points, it is not possible to determine the heat partition factor directly.

The heat partition factor can be then determined by an optimization algorithm with a goal to match the temperature data from the experiment with the downsized model of the wheel and rail with the predicted temperature data generated by functional dependence obtained by Kriging from the virtual experiment. For instance, a multi objective genetic algorithm can be used in order to find an approximate value of the heat partition factor for the specific tribological conditions. The optimization goal was, as already noted, to match the predicted temperatures in eight monitoring points with the experimental ones. By using the noted optimization algorithm, it was determined that the heat partitioning factor was exactly 0.11. It is important to note that the obtained value of the heat partitioning factor was obtained for the time of 1.5 s *i. e.* the final simulation time corresponds to the experiment final time. The obtained result is in agreement with the results obtained by other authors. Thus, Kennedy *et al.* [22] state that most of the heat generated in a sliding wheel-rail contact is transferred into the rail in the way that at the beginning the heat distribution is evenly divided between the wheel and the rail, but over time, almost all of the heat enters the rail. Since temperature data is obtained experimentally for multiple points before the final experiment/simulation time, it is possible to determine the heat partitioning factor in all those points. The main strengths of the new procedure lay in possibility to easily determine values of the heat partitioning factor at different times as well as for different tribological conditions. For instance, the sliding speed and contact pressure can be changed very easily in experimental and numerical part of the procedure.

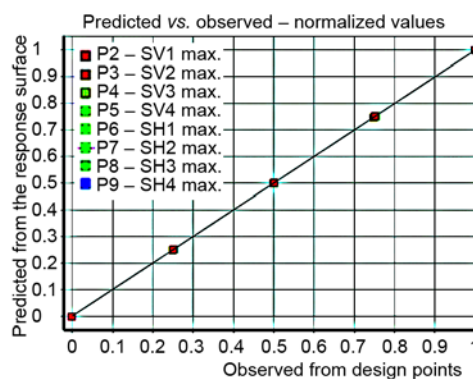


Figure 7. Predicted values of temperature in monitoring points vs. observed temperature data from numerical experiment

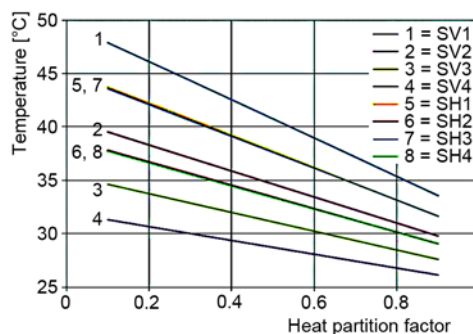


Figure 8. Dependence of temperature in monitoring points from the heat partition factor

Conclusions

The paper presents a new procedure for determination of the heat partition factor in the wheel-rail contact. The procedure combines the results of the experiment on a downsized model of the wheel and the rail and results of the virtual experiment by the finite element analysis in order to determine the exact value of the heat partition factor by the optimization procedure based on matching temperatures obtained by the virtual and the real experiment.

It is determined that the value of the heat partition factor is 0.11 which suggests that most of the generated friction heat is transferred to the rail. This indicates that for responsible mechanical assemblies, special attention should be paid in analyzing the generated friction heat, rather than adopting the default value of 0.5 for the heat partition factor which is mainly offered by modern software simulation packages. The advantage of the new procedure is that the experiment is performed on a simple downsized model of the wheel and rail so that contact tribological parameters can be changed swiftly and with little effort. The new procedure presented in the paper is reasonably straight forward to carry out and can be expanded to account for temperature-dependent thermal properties, radiation and other complexities if needed. The simple and easy determination of the heat partitioning factor enables more accurate simulations of the wheel-rail contact and thus better prediction of RCF and wear.

As the value of the heat partition factor was determined for the pure sliding condition, further research should be directed towards validation of the procedure for the more realistic simultaneous sliding and rolling conditions which occur in the real wheel-rail contact.

Nomenclature

C – specific heat, [$\text{Jkg}^{-1}\text{K}^{-1}$]
 k – thermal conductivity, [$\text{Wm}^{-1}\text{K}^{-1}$]
 p – contact pressure, [Pa]
 \dot{Q} – internal heat generation rate per unit volume, [Wm^{-3}]
 q_t – rate of heat generated per unit area of contact, [Wm^{-2}]
 T – temperature, [K]

t – time, [s]
 v – velocity, [ms^{-1}]

Greek symbols

κ – thermal diffusivity ($=k/\rho C$), [m^2s^{-1}]
 μ – coefficient of friction, [–]
 ρ – density, [kgm^{-3}]

References

- [1] Masoudi Nejad, R., et al., Numerical Study on Fatigue Crack Growth in Railway Wheels under the Influence of Residual Stresses, *Engineering Failure Analysis*, 52 (2015), June, pp. 75-89
- [2] Knothe, K., Liebelt S., Determination of Temperatures for Sliding Contact with Applications for Wheel-Rail Systems, *Wear*, 189 (1995), 1-2, pp. 91-99
- [3] Ertz, M., Knothe, K., A Comparison of Analytical and Numerical Methods for the Calculation of Temperatures in Wheel/Rail Contact, *Wear*, 253 (2002), 3-4, pp. 498-508
- [4] Gallardo-Hernandez, E. A., et al., Temperature in a Twin-Disc Wheel/Rail Contact Simulation, *Tribology International*, 39 (2006), 12, pp. 1653-1663
- [5] Fischer, F. D., et al., Thermal Stresses for Frictional Contact in Wheel-Rail Systems, *Wear*, 211 (1997), 2, pp. 156-163
- [6] Sinha, A. K., et al., Analysis of Thermal Stresses Contact Problem of Functional Material Involving Frictional Heating with and without Thermal Effects, *International Journal of Mechanical And Production Engineering*, 2 (2014), Oct., pp. 42-46
- [7] Belhocine, A., et al., Structural and Contact Analysis of a 3-Dimensional Disc-Pad Model with and without Thermal Effects, *Tribology in Industry*, 36 (2014), 4, pp. 406-418
- [8] Belhocine, A., Bouchetara, M., Thermomechanical Behaviour of Dry Contacts in Disc Brake Rotor with a Grey Cast Iron Composition, *Thermal Science* 17 (2013), 2, pp. 599-609
- [9] Belhocine, A., Bouchetara, M., Thermomechanical Modelling of Dry Contacts in Automotive Disc Brake, *International Journal of Thermal Sciences*, 60 (2012), Oct., pp. 161-170

- [10] Milošević, M., et al., Modeling Thermal Effects in Braking Systems of Railway Vehicles, *Thermal Science* 16 (2012), Suppl. 2, pp. S515-S526
- [11] Stefancu, A. I., et al., Finite Element Analysis of Frictional Contacts, *The Bulletin of the Polytechnic Institute of Jassy, Construction*, 61 (2011), 3, pp. 131-140
- [12] Masoudi Nejad, R., et al., Simulation of Railroad Crack Growth Life under the Influence of Combination Mechanical Contact and Thermal Loads, *Proceedings*, 3rd International Conference on Recent Advances in Railway Engineering (ICRARE 2013), Tehran, 2013
- [13] Salehi, S. M., et al., Life Estimation in the Railway Wheels under the Influence of Residual Stress Field, *International Journal of Railway Research*, 1 (2014), 1, pp. 53-60
- [14] Miltenović, A., et al., Determination of Friction Heat Generation in Wheel-Rail Contact Using FEM, *Facta Universitatis Series: Mechanical Engineering*, 13 (2015), 2, pp. 99-108
- [15] Fischer, F. D., et al., On the Temperature in the Wheel-Rail Rolling Contact, *Fatigue and Fracture of Engineering Materials and Structures*, 26 (2003), 10, pp. 999-1006
- [16] Spiriyagin, M., et al., Numerical Calculation of Temperature in the Wheel-Rail Flange Contact and Implications for Lubricant Choice, *Wear*, 268 (2010), 1, pp. 289-293
- [17] Vakkalagadda, M. R. K., et al., Estimation of Railway Wheel Running Temperatures Using a Hybrid Approach, *Wear*, 328-329 (2015), Apr., pp. 537-551
- [18] Bhusan, B., *Modern Tribology Handbook Volume One Principles of Tribology*, CRC Press LLC, Boca Raton, Fla., USA, 2001
- [19] Yamazaki, H., et al., A Study of Adhesion Force Model for Wheel Slip Prevention Control, *The Japan Society of Mechanical Engineers*, 47 (2004), 2, pp. 469-501
- [20] ***, ANSYS theory manual
- [21] Michael, S., *Interpolation of Spatial Data: Some Theory for Kriging*, Springer Science & Business Media, Springer-Verlag, New York, 1999
- [22] Kennedy, T. C., et al., Transient Heat Partition Factor for a Sliding Railcar Wheel, *Wear*, 261 (2006), 7, pp. 932-936

